DMD Fast Forward. Published on May 19, 2023 as DOI: 10.1124/dmd.122.001194
This article has not been copyedited and formatted. The final version may differ from this version.

Systemic Exposure, Metabolism, and Elimination of [^{14}C]-Labeled Amino Lipid, Lipid 5, After a Single Administration of mRNA Encapsulating Lipid Nanoparticles to Sprague Dawley Rats

Douglas Burdette, Lei Ci, Barclay Shilliday, Richard Slauter[1], Andrew Auerbach, Matthew Kenney, Örn Almarsson, Eugene Cheung, Tracy Hendrick

Moderna, Inc., Cambridge, Massachusetts (DB, LC, AA, MK, and EC)

Charles River Laboratories, Mattawan, Michigan (BS and RS)

Duke University, Durham, North Carolina, USA (TH)

Lyndra Therapeutics, Cambridge, Massachusetts, USA (OA)

Primary laboratory of origin: Moderna, Inc.

DMD Fast Forward. Published on May 19, 2023 as DOI: 10.1124/dmd.122.001194
This article has not been copyedited and formatted. The final version may differ from this version.

Running title: Lipid 5 Exposure, Metabolism, and Elimination in Rats

Corresponding author:

Douglas Burdette

Moderna, Inc.

200 Technology Square

Cambridge, MA 02139, USA

Telephone: 617-218-7613

E-mail: Doug.Burdette@modernatx.com

Number of text pages: 21

Number of tables: 0

Number of figures: 5

Number of references: 16

Number of words in the Abstract: 234

Number of words in the Introduction: 557

Number of words in the Discussion: 1557

Abbreviations

ADME, absorption, distribution, metabolism, and excretion

AUC_{last}, area under the concentration-time curve to the last measurable concentration

C_{max}, maximum concentration

DMSO, dimethyl sulfoxide

HPLC-RAD, high-performance liquid chromatography with radioactivity detection

DMD Fast Forward. Published on May 19, 2023 as DOI: 10.1124/dmd.122.001194
This article has not been copyedited and formatted. The final version may differ from this version.

HRMS, high-resolution mass spectrometry

IV, intravenous

LNP, lipid nanoparticle

mRNA, messenger ribonucleic acid

MS, mass spectrometry

NHP, nonhuman primate

NTFIX, non-translating Factor IX

PEG, polyethylene glycol

PK, pharmacokinetic

RNA, ribonucleic acid

DMD Fast Forward. Published on May 19, 2023 as DOI: 10.1124/dmd.122.001194
This article has not been copyedited and formatted. The final version may differ from this version.

ABSTRACT

The emerging therapeutic modality of lipid nanoparticle (LNP)-encapsulated mRNAs has demonstrated promising clinical results when used as vaccines and is currently being tested in formulations for a wide range of targeted chronic disease treatments. These therapeutics are multicomponent assemblages of well-characterized naturally occurring molecules in addition to xenobiotic molecules, whose in vivo distributions are poorly understood. Here, the metabolic outcome and in vivo elimination of Lipid 5, a key xenobiotic amino lipid in LNP formulations, were assessed after intravenous administration of ^{14}C-labeled Lipid 5 to Sprague Dawley rats. Intact Lipid 5 was predominantly cleared from plasma within 10 h after dosing, with only small quantities (<1% of ^{14}C dose) of a single diacid metabolite detected after 10 h. Lipid 5 was rapidly metabolized via ester hydrolysis into aliphatic alcohols and diacidic amino head group moieties, which were further metabolized via β-oxidation. Overall, >90% of the administered Lipid 5-derived ^{14}C was recovered in urine (65%) and feces (35%), predominantly as oxidative metabolites, within 72 h after dosing, indicating rapid renal and hepatic elimination. In vitro metabolite identification after incubation with human, nonhuman primate, and rat hepatocytes showed similar metabolites to those found in vivo. No meaningful differences were observed in Lipid 5 metabolism or elimination by sex. In conclusion, Lipid 5, a critical amino lipid component of LNPs for mRNA therapeutic delivery, showed minimal exposure, rapid metabolism, and near-complete elimination of ^{14}C metabolites in rats.

DMD Fast Forward. Published on May 19, 2023 as DOI: 10.1124/dmd.122.001194
This article has not been copyedited and formatted. The final version may differ from this version.

SIGNIFICANCE STATEMENT

Lipid 5 is a key component of lipid nanoparticles used for the delivery of mRNA-based medicines; understanding the rates and routes of its clearance is crucial to assessing its long-term safety in LNP technology. This study conclusively established the rapid metabolism, and near-complete elimination of intravenously administered [^{14}C]Lipid 5 in rats via both liver and kidney as oxidative metabolites derived from ester hydrolysis and subsequent β-oxidation.

DMD Fast Forward. Published on May 19, 2023 as DOI: 10.1124/dmd.122.001194
This article has not been copyedited and formatted. The final version may differ from this version.

INTRODUCTION

RNA represents a novel and expanding class of human therapeutic modalities. The demonstration that RNAs may be protected from degradation in vivo by encapsulation in lipid nanoparticles (LNPs) and that these LNPs can effectively deliver biologically active RNAs into target cells has enabled them to be adapted for use as human therapeutics (Berraondo et al., 2019; Foster et al., 2019; Gan et al., 2019; Zhang et al., 2019). Because RNA sequences are unique and can recognize specific complementary nucleic acid sequences, specifically interact with proteins, or be translated into specific proteins within cells, they may be designed with exquisite selectivity to target a range of molecular disease mechanisms. LNPs typically consist of multiple components, including an ionizable lipid, a phospholipid, a sterol, and a PEG-lipid (Hassett et al., 2019). These molecular components are initially distributed as intact particles but may have separate metabolic outcomes after the LNP delivers its RNA payload.

Therapeutic mRNAs pose additional design challenges related to their large size (10^5–10^6 Da), in vivo distribution, and the productive delivery of LNP-encapsulated mRNA into target cells for therapeutic protein translation (Patel et al., 2017). Studies have demonstrated that mRNA biodistribution generally aligns with that of other assessed LNP components (Ci et al., in preparation). Notably, such observations stem from studies of mRNA-containing LNPs as acute treatments or as vaccines. Consequently, any safety concerns regarding the distribution of LNP components have been addressed in alignment with guidance for acute dosing (FDA, 2013). However, because mRNA-containing LNPs are being considered for the treatment of chronic conditions and use in various clinical subpopulations (e.g., pediatric or renally- and hepatically-impaired individuals), further understanding how LNP components are processed, including how

DMD Fast Forward. Published on May 19, 2023 as DOI: 10.1124/dmd.122.001194
This article has not been copyedited and formatted. The final version may differ from this version.

they influence mRNA delivery and therapeutic protein expression, can influence predictions of exposure and risk.

It has generally been assumed that LNP components are processed and eliminated via endogenous pathways based on their biochemical classification (e.g., lipid or RNA). Although therapeutic mRNAs include modified uridine to avoid innate immune stimulation (Nelson et al., 2020), this modification is naturally occurring and its use has not been linked to any specific safety concerns (EMA, 2021). Additionally, the inactivation of therapeutic mRNAs via endo- and exonuclease activity has been established (Steinle et al., 2017; Hou et al., 2021). Naturally occurring lipids such as cholesterol, and cholesterol esters, in non-native particles (e.g., LNPs) are expected to be biologically processed similar to their endogenous analogs. Lipid and cholesterol esters that combine naturally occurring molecules with well-known xenobiotic lipids (e.g., PEGs) via labile linkages also appear to be processed as individual components after primary metabolism via hydrolysis (Webster et al., 2007). Lipid 5, a xenobiotic amino lipid used in mRNA-encapsulating LNPs is comprised of an ethanolamine ionizable head group with primary ester-containing lipid tails (Sabnis et al., 2018). However, exposure to these xenobiotic LNP components (Ci et al., in preparation), their processing after hydrolysis, and the appropriate means to assess these metabolites remains an area of active research and discussion.

Although the outcome of naturally occurring LNP components may be reliably described by endogenous physiological processes, the predicted behavior and in vivo interactions of xenobiotic portions of LNP components, such as Lipid 5, remain unknown. Here, the in vivo metabolic outcome and elimination of Lipid 5 were determined in Sprague Dawley rats, a well-established preclinical pharmacokinetic (PK) and absorption, distribution, metabolism, and excretion (ADME) model.

DMD Fast Forward. Published on May 19, 2023 as DOI: 10.1124/dmd.122.001194
This article has not been copyedited and formatted. The final version may differ from this version.

MATERIALS AND METHODS

Reagents. The heptadecan-9-yl 8-((2-hydroxyethyl) (8-(nonyloxy)-8-oxooctyl)amino)octanoate (Lipid 5) used in the studies described here was synthesized as described previously (Sabnis et al., 2018) with ^{14}C at the proximal carbon of the ethanolamine aliphatic chain that was linked to the tertiary nitrogen and purified to 95% chemical (99%) radioactivity for incorporation into LNPs. [^{14}C]Lipid 5-containing LNPs that encapsulated a single, nontranslating Factor IX (NTFIX) mRNA were formulated as described previously (Sabnis et al., 2018).

In Vitro Model. Lipid 5-containing LNPs encapsulating NTFIX mRNA were incubated in the presence of pooled, cryopreserved human (5 males/5 females), male non-human primate (NHP), or male rat hepatocytes (10^6 cells/mL in William's E medium supplemented with GlutaMAX-1 (2 mM) and HEPES (0.1 mM) in 0.250-mL incubation volume) at 10 mM encapsulated mRNA at 37 °C in the presence of 95% relative humidity and 5% CO_2 for up to 240 min compared to incubations with heat-inactivated hepatocytes. The reactions were terminated by the addition of an equal volume of acetonitrile and centrifuged (920×*g* for 10 min at 10 °C) to recover the supernatant for metabolite identification. 7-Ethoxycoumarin (500 μM, final concentration) was used as a positive control substrate to evaluate the metabolic competency of the hepatocytes.

Animal Model. Two groups of six male and six female adult (8-10 weeks, 250 g – 350 g) Sprague Dawley rats (FVC) were dosed via 10 min IV infusion with [^{14}C]Lipid 5-containing LNP encapsulating a single, NTFIX mRNA (Eurofins, St. Louis, MO) at 2 mg/kg (3.3 mL/kg). All research involving animals was conducted at Charles River Laboratories (CRL) in accordance with CRL-Mattawan and Moderna, Inc. Animal Care and Use Committee guidelines.

DMD Fast Forward. Published on May 19, 2023 as DOI: 10.1124/dmd.122.001194
This article has not been copyedited and formatted. The final version may differ from this version.

Sample Preparation. Plasma samples were prepared from serial bleeds collected from unanaesthetized animals at either 0.083, 0.5, 2, 6, 24, and 48 hours post dose or 0.25, 1, 4, 10, 36, and 168 hours post dose (3 males /3 females) per subgroup. Plasma samples were processed by protein precipitation with a 6× volume of acetonitrile:methanol (1:1). After centrifugation, the pellets were extracted again with acetonitrile:methanol (1:1). The supernatants were combined and concentrated to dryness by vacuum centrifugation. The residues were reconstituted in 400 µL dimethyl sulfoxide (DMSO) followed by 800 µL acetonitrile/isopropanol and 800 µL water. Urine samples were prepared from urine specimens collected before dosing and 0–8 h, 8–24 h, and 24–168 h after dosing by combining equal percentages of each sample by weight. Samples were analyzed directly by high-performance liquid chromatography with radioactivity detection/high-resolution mass spectrometry (HPLC-RAD/HRMS). Fecal homogenate pools were prepared from homogenized samples collected before dosing and 0–8 h, 8–24 h, 24–48 h, 48–72 h, and 168 h after dosing. Aliquots of each pool, 2 g each, were extracted with 10 mL acetonitrile;isopropanol (1:1). After centrifugation, the pellets were extracted again with acetonitrile:isopropanol (1:1). The supernatants were then combined and concentrated to dryness in a vacuum centrifuge at 40 °C. The residues were reconstituted in 400 µL DMSO, followed by the addition of 800 µL acetonitrile:isopropanol (1:1) and 800 µL water.

Cages were rinsed with deionized water at 24, 48, 72, 96, 120, 144, and 168 hours post dose with an additional rinse including 1% TSP at 168 h post dose. Following the final excreta collection and final cage rinse with 1% TSP, the interior aspect of each cage was wiped with a gauze sponge. Cage wipes were extracted overnight in deionized water and the total sample weight determined. Following thorough mixing, these samples were aliquoted in triplicate for radioactivity analysis by liquid scintillation counting (LSC).

DMD Fast Forward. Published on May 19, 2023 as DOI: 10.1124/dmd.122.001194
This article has not been copyedited and formatted. The final version may differ from this version.

HPLC-RAD and Mass Spectrometry Detection. Radio-HPLC analyses were performed using an Agilent 1200 ultra-performance liquid chromatography system (Agilent Technologies Inc., Santa Clara, CA) with a 96-well Collect PAL fraction collector (Leap Technologies, Carrboro, NC). Radioactivity in the effluent was monitored using an IN/US β-Ram Model 5B Radio-HPLC detector (LabLogic, Tampa, FL) with continuous flow through a 500-µL cell. Prior to entering the radioactive flow detector, the column effluent was mixed with Ultima-Flo M scintillation cocktail (PerkinElmer, Waltham, MA) at a rate of 1.6 mL/min. Radiochromatograms were integrated by manually selecting peaks substantially above baseline using the Laura™ software package (LabLogic Systems Inc., Tampa, FL). Chromatography was performed on an Kinetix XB-C-18 column, 4 µm particle size, 4.6 × 150 mm (Phenomenex Inc., Torrance, CA) at 40 °C. Mobile phase A consisted of formic acid (0.1% v/v) in water, whereas mobile phase B consisted of formic acid (0.1% v/v) in acetonitrile:isopropanol (1:1, v/v.). Gradient elution was used at a flow rate of 1 mL/min and was split after column with 80% diverted to radiodetector and 20% to the mass spectrometer.

Orbitrap Mass Spectrometry. Positive ion detection mode was employed on an LTQ Discovery XL mass spectrometer (Thermo Fisher, Waltham, MA). The electrospray ionization source parameters were as follows: spray voltage, 4.0 kV; capillary temperature, 400 °C; source heater temperature, 400 °C; sheath gas, 40 arbitrary units; auxiliary gas, 10 arbitrary units; sweep gas, 5 arbitrary units. Full scan data were collected at 15,000× resolution. Targeted tandem mass spectrometry experiments were performed during subsequent injections using collision-induced dissociation at a collision energy of 25 eV. Data were acquired using Xcalibur software (version 2.1; Thermo Fisher, Waltham, MA).

DMD Fast Forward. Published on May 19, 2023 as DOI: 10.1124/dmd.122.001194
This article has not been copyedited and formatted. The final version may differ from this version.

RESULTS

In Vitro Metabolite Identification. Incubation of Lipid 5 with rat, NHP, and human hepatocytes led to the development of four metabolites, namely, monoacid and diacid ethanolamine head group metabolites resulting from ester cleavage of the fatty acid chains and diacid head group metabolites with the aliphatic acid chain shortened by four carbons (**Figure 1**). The monoacid forms include the branched chain with the straight chain eliminated. Two diacid metabolites were identified with either full-length (eight-carbon) linkers or with one linker being shortened by four carbons. Based on these results, the ^{14}C that was on the ethanolamine aliphatic chain linked to the tertiary nitrogen allowed tracking of the head group portion of the molecule for subsequent in vivo analysis (**Figure 1**).

Pharmacokinetics and Mass Balance. Plasma ^{14}C levels after IV infusion of [^{14}C]Lipid 5-containing LNPs encapsulating NTFIX mRNA (2 mg/kg) decreased rapidly within the first 6 h after dosing ($T_{1/2}$ = 8.42-9.04 h); plasma ^{14}C levels were <0.1% of C_{max} within 24 h and persisted in low levels before reaching trace levels by 48 h after dosing (**Figure 2A**). Analysis of plasma PK data suggested the presence of an initial distribution phase followed by a single-phase terminal clearance. While modestly higher Cmax and AUC values were determined for females in this study, the male and female exposures follow the same time course and the numbers observed are within the acceptable range of data variability indicating that no meaningful differences by sex were observed in either the extent or dynamics of exposure. After a single IV administration of a therapeutic LNP of identical composition but containing unlabeled Lipid 5, the plasma concentration of unlabeled Lipid 5 decreased to <1% of its C_{max} value within 24 h after dosing ($T_{1/2}$ = 1.4 h; Fig. 2B), similar to PK observed when using [^{14}C]Lipid 5. Accounting

DMD Fast Forward. Published on May 19, 2023 as DOI: 10.1124/dmd.122.001194
This article has not been copyedited and formatted. The final version may differ from this version.

for the estimated 7.5% [^{14}C]Lipid 5 relative to total Lipid 5, the AUC_{last} value in this study (352,000 ng/mL*h) was also comparable to that for the therapeutic LNP (522,000 ng/mL*h).

Feces and urine collected from the same animals were analyzed for radioactivity (**Figure 3**). After 168 h, >90% of the administered radioactivity was recovered in feces and urine. Most radioactivity was recovered in urine (61.8% ± 4.0%) within the first 24 h after dosing, with 42.9% ± 6.6% recovered within the first 8 h. Total fecal radioactivity was slightly higher in females (25.0% ± 1.6%) than males (20.4% ± 1.8%), with 18.4% ± 2.0% and 16.2% ± 3.4% recovery within the first 48 h in males and females, respectively.

In Vivo Metabolite Identification. Plasma, urine, and fecal samples from the mass balance study in Sprague Dawley rats were analyzed for the presence of [^{14}C]Lipid 5 metabolites. The structures of the most abundant metabolites, including all metabolites that represented at least 10% of the dosed [^{14}C]Lipid 5 (M5, M7, M10-M14, M17, and M18), were determined. The structures of less abundant metabolites (M1-M4, M6, M8, M9, M15, and M16) were not determined. At 1 h after dosing, plasma contained mainly Lipid 5 and diacid ester hydrolysis metabolites with either no further carbon chain shortening (M14) or a four-carbon chain-length reduction in one linker (M11) (Fig. 4). Additionally, monoacidic [^{14}C]Lipid 5 metabolites containing the branched aliphatic chain with either no further carbon chain shortening (M18) or a four-carbon chain-length reduction in the straight chain linker (M17) were detected. By 10 h after dosing, no intact Lipid 5 was detected in plasma, and the only [^{14}C]Lipid 5 metabolite detected was the diacid with a four-carbon chain-length reduction in both chain linkers (M5) (**Figure 4**).

No intact Lipid 5 was detected in urine at either the 0–8 h or 8–24 h postdose intervals (**Figure 5A**). A number of diacid [^{14}C]Lipid 5 metabolites were detected in urine from both

DMD Fast Forward. Published on May 19, 2023 as DOI: 10.1124/dmd.122.001194
This article has not been copyedited and formatted. The final version may differ from this version.

males and females at similar relative amounts at the earlier time interval (M5–M7 and M9–M14); however, by 8–24 h after dosing, urine from both males and females contained three predominant diacid metabolites: the hydrolyzed ester metabolite with no further carbon chain shortening (M14), a four-carbon chain-length reduction in one linker (M11), and a four-carbon chain-length reduction in both linkers (M5; **Figure 5A**). Also, the relative amounts of the three diacids shifted toward the smaller M5 metabolite in the later sample pool.

No metabolite identification data were obtained for fecal samples before 8 h after dosing due to the low level of radioactivity present in these samples. By 8–24 h after dosing, no intact [^{14}C]Lipid 5 was detected in feces, and the predominant species present were the diacids with either no further carbon chain shortening (M14) or a four-carbon chain-length reduction in one linker (M11; **Figure 5B**). The monoacidic [^{14}C]Lipid 5 metabolites containing the branched aliphatic chain with either no further carbon chain shortening (M18) or a four-carbon chain-length reduction in the straight chain linker detected in plasma and the diacid with a four-carbon chain-length reduction in both linkers (M5) detected in urine were also identified in feces. Additionally, metabolites with masses consistent with hydrolysis of the branched aliphatic chain with (M15, m/z = 502.3727 [$C_{27}H_{51}NO_7$]) and without β-oxidation (M16, m/z = 530.4048 [$C_{29}H_{55}NO_7$]) were detected at chromatographic retention times consistent with monoacid identification. However, due to their low ^{14}C abundance, structural determination from the samples was not performed. No differences by sex were observed in these fecal metabolite profiles.

DMD Fast Forward. Published on May 19, 2023 as DOI: 10.1124/dmd.122.001194
This article has not been copyedited and formatted. The final version may differ from this version.

DISCUSSION

LNP-encapsulated mRNAs are a promising, novel class of therapeutics. LNPs consist of multiple components, with the lipids exerting a significant influence on the in vivo distribution and productive cellular delivery of encapsulated mRNAs. The lipid components of the LNP consist of both naturally occurring and xenobiotic chemicals. The in vivo disposition of the naturally occurring molecules follow the routes established for their endogenous counterparts. In this study, using well-established, quantitative drug metabolism and PK techniques, LNPs containing ^{14}C-labelled Lipid 5 were administered to rats, and [^{14}C]Lipid 5 outcome was monitored over time. In vitro metabolite identification using human, NHP, and rat hepatocytes indicated that the metabolism and elimination of a critical LNP component followed established ADME principles and were predictable by applying in vivo biochemical understanding based on its chemical structure.

Rational assessment of the probable sites of Lipid 5 metabolism suggested that the esters linking the single and branched aliphatic chains would be labile and the liberated aliphatic alcohols oxidized to fatty acids and processed accordingly. Because the potential outcome of the ethanolamine linker portion of the molecule was less clear, the ^{14}C radiolabel was incorporated on that portion of the molecule to assist in tracking its metabolism and elimination. In vitro incubation with human, NHP, and rat hepatocytes resulted in ester hydrolysis of both straight and branched aliphatic chains and four-carbon shortening of the acid linker to the liberated straight chain in all species tested. The absence of a straight chain monoacidic metabolite and the presence of both monoacid and diacid metabolites with four-carbon shortening of the straight chain linker indicates that the branched chain ester was more biochemically stable than the straight chain ester and that linker shortening occurred after ester hydrolysis, likely via β-

DMD Fast Forward. Published on May 19, 2023 as DOI: 10.1124/dmd.122.001194
This article has not been copyedited and formatted. The final version may differ from this version.

oxidation (reviewed in (Houten and Wanders, 2010)). No metabolism on the ethanolamine portion of the Lipid 5 head group was identified; thus, adding the ^{14}C label on the ethanolamine provided a robust reporter of the entire Lipid 5 head group in vivo.

After the administration of [^{14}C]Lipid 5-containing LNPs containing NTFIX mRNA to Sprague Dawley rats, Lipid 5 monoacid and diacid metabolites and intact Lipid 5 were rapidly detected in plasma. Levels of all ^{14}C species decreased rapidly over 24 h after dosing with no detectable Lipid 5 and only one diacid, shortened-linker metabolite (M5) detected in plasma after 10 h. Note that the persistence of low level radioactivity in plasma from 12 to 48 h after dosing compared to the rapid loss of intact Lipid 5 in the unlabeled Lipid 5 study is consistent with the appearance of Lipid 5 metabolites after the rapid disappearance of intact Lipid 5 in circulation. In vivo detection of the monoacid metabolites (M17 and M18) indicates that the straight chain ester was more rapidly hydrolyzed than the branched chain ester, similar to observations made from in vitro studies. These monoacids that are pathway intermediates in generating the shorter monoacidic and di-acidic metabolites seen across genders were detected only in female rats at the 1 h post dose timepoint, suggesting differential hydrolysis rates between female and male rats. However, the modest number of animals included in this experiment caution against overinterpreting minor differences between sexes. Additionally, the alignment of the identities and levels of diacid metabolites at 1 h and 10 h after dosing as well as the very similar metabolite identities and levels seen in excreta provide no evidence for mechanistic differences in Lipid 5 metabolism between males and females. The presence of diacid metabolites M14 and M11 in plasma at 1 h after dosing and M5 at 10 h after dosing suggested that, following ester hydrolysis, β-oxidation occurred in a stepwise fashion on each linker independently. Also, four-carbon chain-length reduction to four-carbon acids on the headgroup linkers appears to be the primary

DMD Fast Forward. Published on May 19, 2023 as DOI: 10.1124/dmd.122.001194
This article has not been copyedited and formatted. The final version may differ from this version.

terminal metabolic product. Finally, while metabolite M5 was present at 10 h after dosing, after Lipid 5 was no longer detectable, pharmacokinetic monitoring of total ^{14}C demonstrated little residual radioactivity by 24 h after dosing, indicating that Lipid 5-derived material did not persist at significant levels in circulation beyond one day.

Radiolabeled material in urine from males and females in both the 0–8 h and 8–24 h post dose pools included only diacid metabolites, with no detectable monoacid metabolites or intact Lipid 5, indicating that only small, highly charged species were eliminated via the kidneys. The chemical stability of Lipid 5 in urine was confirmed to ensure that the lack of Lipid 5 detected in urine did not result from chemical hydrolysis in the samples (data not shown). The mass balance data demonstrate that these diacid metabolites represent elimination of most Lipid 5 headgroup material in urine and that Lipid 5 excretion occurred predominantly within the first 24 h after dosing. Although the highly polar metabolites M1–M4 were detected in urine at low levels, they were not detected in plasma, indicating that they did not contribute to systemic exposure by Lipid 5 metabolites, and their structures were not elucidated. While the presence of metabolites in urine not detected in plasma may result from uniquely renal metabolism, they may also result from Lipid 5 diacid metabolites formed outside of the kidneys that were rapidly renally eliminated, reducing their circulating levels below the level of detection.

Feces contained a broader range of metabolites, including larger, more lipophilic monoacids but no detectable intact Lipid 5. The major monoacid metabolites resulted from straight aliphatic chain ester hydrolysis with and without subsequent linker β-oxidation but did not include monoacids with hydrolysis of the branched aliphatic chain. These results demonstrated that the straight chain ester was sufficiently more biochemically labile than the branched chain ester and allowed for linker β-oxidation and secretion into bile before the

DMD Fast Forward. Published on May 19, 2023 as DOI: 10.1124/dmd.122.001194
This article has not been copyedited and formatted. The final version may differ from this version.

branched chain was hydrolyzed. Minor metabolite peaks (M15 and M16) at reverse-phase HPLC retention times between those of the branched chain-containing monoacids and diacids with full-length eight-carbon linkers (M14) had masses consistent with hydrolysis of the branched chain, indicating the existence of monoacidic metabolites with the straight chain intact. These data align with the conclusion that monoacid metabolites with either aliphatic chain cleaved were present and that the straight chain was more susceptible to hydrolysis, as would be expected based on steric considerations. Several diacidic metabolites were also present in feces (M5, M11, M13, and M14) and displayed various degrees of linker β-oxidation with no evidence of metabolism beyond four-carbon linkers (M5) and no evidence of metabolism on the ethanolamine portion of the headgroup. Applying similar logic to that for M15 and M16 based on bracketed reverse-phase HPLC retention times, M10 could represent another diacidic species present in feces. However, structural elucidation was not performed due to its low abundance so this hypothesis cannot be confirmed.

Lipid 5 introduced as a component of mRNA-containing complex LNP was extensively metabolized and the resulting oxidative metabolites were efficiently eliminated via hepatic and renal routes within 24 h of IV administration. The primary routes of Lipid 5 metabolism were consistent with rational predictions based on its chemical structure and probable interactions with common biochemical pathways. The absence of detectable Lipid 5 in both feces or urine and the highly polar nature of the circulating and secreted metabolites does not support the proposal that Lipid 5 elimination occurs as part of intact LNPs but rather that it occurs after metabolism and secondary distribution of these polar metabolites, independent of the administered LNP.

Mass balance analysis showed that >80% of radioactivity was recovered in urine and feces within 24 h after dosing and >90% within 168 h, almost exclusively as hydrolytic and β-

DMD Fast Forward. Published on May 19, 2023 as DOI: 10.1124/dmd.122.001194
This article has not been copyedited and formatted. The final version may differ from this version.

oxidative metabolites, which indicates that these excreted metabolites represent the bulk of the dosed [^{14}C]Lipid 5. The identities of these metabolites were consistent with expectations based on established biotransformation pathways for Lipid 5 in isolation, indicating that established biotransformation principles for small molecules may be applied to the prediction of the metabolic outcomes of LNP component lipids. The renal elimination of small, diacid Lipid 5 head group metabolites via renal and a broader cross-section of monoacid and diacid metabolites via the liver were consistent with established principles for small molecule elimination via these routes (Varma et al., 2009; Varma et al., 2012). Therefore, metabolism and elimination principles that are well-established for small molecules may be applied in predicting the in vivo disposition of LNP-delivered Lipid 5.

In summary, this study provided experimentally sensitive ^{14}C-labeling strategies for monitoring Lipid 5 metabolism and elimination using both in vitro hepatocytes and in vivo rat models. The experimental design also provided assessment of sex-based differences on Lipid 5 metabolism and elimination. Data presented here suggest that the mRNA encapsulating LNPs do not persist in vivo and that the novel amino lipid component, Lipid 5, is efficiently cleared by multiple, well-established routes. The metabolites identified in circulation and excreta are consistent with biotransformation via ubiquitous, high-capacity pathways shared by rodents, non-human primates, and humans already established for similar small molecules, suggesting that Lipid 5 metabolism is not influenced by LNP delivery. The application of ADME principles established for small molecules to accurately predict the in vivo disposition of Lipid 5 by pathways consistent with its chemical identity alone suggests that these principles may be applied more generally to the components of these complex biotherapeutics. This study provides further evidence for the safe use of LNP technology for the delivery of mRNA-based medicines.

DMD Fast Forward. Published on May 19, 2023 as DOI: 10.1124/dmd.122.001194
This article has not been copyedited and formatted. The final version may differ from this version.

ACKNOWLEDGMENTS

Medical writing and editorial assistance were provided by Jared Cochran, PhD, and Wynand van Losenoord, MSc, of MEDiSTRAVA in accordance with Good Publication Practice (GPP3) guidelines, funded by Moderna, Inc., and under the direction of the authors. The authors acknowledge the Moderna colleagues Kerry Benenato, Greg Mercer, Don Parsons, and John Joyal for critical coordination and insightful discussion related to this work and the Eurofins teams responsible for synthesizing and characterizing [^{14}C]Lipid 5 and the ^{14}C-containing LNPs.

AUTHOR CONTRIBUTIONS

Participated in research design: Burdette, Ci, Auerbach, Kenney, Almarsson, Cheung and Hendrick.

Performed data analysis: Shilliday and Slauter.

Wrote or contributed to the writing of the manuscript: Burdette, Ci, Shilliday, Slauter, Auerbach, Kenney, Almarsson, Cheung, Hendrick.

CONFLICT OF INTEREST

DB, LC, AA, MK, and EC are employees of Moderna, Inc. and hold stock/stock options in the company; BS, TH, OA, and RS have no conflicts of interest to declare

DATA SHARING STATEMENT

The authors declare that the data supporting the findings of this study are available within this article.

DMD Fast Forward. Published on May 19, 2023 as DOI: 10.1124/dmd.122.001194
This article has not been copyedited and formatted. The final version may differ from this version.

REFERENCES

Berraondo P, Martini PGV, Avila MA, and Fontanellas A (2019) Messenger RNA therapy for rare genetic metabolic diseases. *Gut* **68:**1323–1330.

EMA (2021) Assessment Report: COVID-19 Vaccine Moderna. https://www.ema.europa.eu/en/documents/assessment-report/spikevax-previously-covid-19-vaccine-moderna-epar-public-assessment-report_en.pdf. Accessed November 16, 2021.

FDA (2013) Guidance Document: Preclinical Assessment of Investigational Cellular and Gene Therapy Products -Guidance for Industry. https://www.fda.gov/regulatory-information/search-fda-guidance-documents/preclinical-assessment-investigational-cellular-and-gene-therapy-products. Accessed February 4, 2022.

Foster JB, Barrett DM, and Kariko K (2019) The emerging role of in vitro-transcribed mRNA in adoptive T cell immunotherapy. *Mol Ther* **27:**747–756.

Gan LM, Lagerstrom-Fermer M, Carlsson LG, Arfvidsson C, Egnell AC, Rudvik A, Kjaer M, Collen A, Thompson JD, Joyal J, et al. (2019) Intradermal delivery of modified mRNA encoding VEGF-A in patients with type 2 diabetes. *Nat Commun* **10:**871.

Hassett KJ, Benenato KE, Jacquinet E, Lee A, Woods A, Yuzhakov O, Himansu S, Deterling J, Geilich BM, Ketova T, et al. (2019) Optimization of lipid nanoparticles for intramuscular administration of mRNA vaccines. *Mol Ther Nucleic Acids* **15:**1–11.

Hou X, Zaks T, Langer R, and Dong Y (2021) Lipid nanoparticles for mRNA delivery. *Nat Rev Mater* **6:**1–17.

Houten SM and Wanders RJ (2010) A general introduction to the biochemistry of mitochondrial fatty acid beta-oxidation. *J Inherit Metab Dis* **33:**469–477.

Nelson J, Sorensen EW, Mintri S, Rabideau AE, Zheng W, Besin G, Khatwani N, Su SV, Miracco EJ, Issa WJ, et al. (2020) Impact of mRNA chemistry and manufacturing process on innate immune activation. *Sci Adv* **6:**eaaz6893.

Patel S, Ashwanikumar N, Robinson E, DuRoss A, Sun C, Murphy-Benenato KE, Mihai C, Almarsson O, and Sahay G (2017) Boosting intracellular delivery of lipid nanoparticle-encapsulated mRNA. *Nano Lett* **17:**5711–5718.

Sabnis S, Kumarasinghe ES, Salerno T, Mihai C, Ketova T, Senn JJ, Lynn A, Bulychev A, McFadyen I, Chan J, et al. (2018) A novel amino lipid series for mRNA delivery: improved endosomal escape and sustained pharmacology and safety in non-human primates. *Mol Ther* **26:**1509–1519.

Steinle H, Behring A, Schlensak C, Wendel HP, and Avci-Adali M (2017) Concise review: application of in vitro transcribed messenger RNA for cellular engineering and reprogramming: progress and challenges. *Stem Cells* **35:**68–79.

Varma MV, Chang G, Lai Y, Feng B, El-Kattan AF, Litchfield J, and Goosen TC (2012) Physicochemical property space of hepatobiliary transport and computational models for predicting rat biliary excretion. *Drug Metab Dispos* **40:**152701537.

Varma MV, Feng B, Obach RS, Troutman MD, Chupka J, Miller HR, and El-Kattan A (2009) Physicochemical determinants of human renal clearance. *J Med Chem* **52:**4844-4852.

Webster R, Didier E, Harris P, Siegel N, Stadler J, Tilbury L, and Smith D (2007) PEGylated proteins: evaluation of their safety in the absence of definitive metabolism studies. *Drug Metab Dispos* **35:**9–16.

Zhang C, Maruggi G, Shan H, and Li J (2019) Advances in mRNA vaccines for infectious diseases. *Front Immunol* **10:**594.

DMD Fast Forward. Published on May 19, 2023 as DOI: 10.1124/dmd.122.001194
This article has not been copyedited and formatted. The final version may differ from this version.

FOOTNOTES

This work was supported by Moderna, Inc.

Person to receive reprint requests

Douglas Burdette, Ph.D.

Moderna, Inc.

200 Technology Square

Cambridge MA 02139

dburdette@modernatx.com

Numbered footnotes

[1]Current affiliation: Microbion Corp., Bozeman, Montana

DMD Fast Forward. Published on May 19, 2023 as DOI: 10.1124/dmd.122.001194
This article has not been copyedited and formatted. The final version may differ from this version.

FIGURE LEGENDS

Figure 1. Lipid 5 metabolite identification scheme. Metabolites included those with >1% abundance relative to dose in plasma, urine, or feces. Lipid 5 and all metabolites identified in vitro after incubation with human, NHP, and rat hepatocytes (all metabolites were detected in all three species) are identified by the designation "heps."

Figure 2. Plasma profiles of [^{14}C] Lipid 5 and unlabeled Lipid 5 after IV administration of [^{14}C] Lipid 5 or unlabeled Lipid 5-containing LNPs to Sprague Dawley rats at 2 mg/kg. (A)^{14}C after single-dose IV administration of [^{14}C]Lipid 5-containing LNPs or (B) unlabeled Lipid 5-containing LNPs to Sprague Dawley rats. Mean values ± standard deviation are represented by squares (males) and circles (females). SD, single dose.

[a]Earliest time point taken in the study.

Figure 3. Excreta mass balance of ^{14}C recovered in male and female rats. (A) urine pooled 0–8 and 8–24 h after dosing including the 24 h post dose cage rinse, (B) feces pooled 0–8, 8–24, 24–48, and 48–72 h after dosing and (**C**) total urine and feces pooled including cage rinse and wipe within 168 h after dosing.

Figure 4. Relative quantitation of [^{14}C]Lipid 5 and related metabolites detected in rat plasma. [^{14}C]Lipid 5 and related metabolites in rat plasma at 1 and 10 h after dosing. Proposed β-oxidation (blue) and ester hydrolysis (red) pathways are shown between parent and daughter chemical species.

DMD Fast Forward. Published on May 19, 2023 as DOI: 10.1124/dmd.122.001194
This article has not been copyedited and formatted. The final version may differ from this version.

Figure 5. Relative quantitation of [^{14}C]Lipid 5 and related metabolites detected in rat urine and feces*. (A) [^{14}C]Lipid 5 and related metabolites in rat urine pooled 0–8 and 8–24 h after dosing. 1 and 10 h after dosing; and (B) [^{14}C]Lipid 5 and related metabolites in rat feces pooled 8–24 h after dosing. Proposed β-oxidation (blue) and ester hydrolysis (red) pathways are shown between parent and daughter chemical species.

*Only sample pools containing significant radioactivity were assessed and therefore, no analysis was performed on the fecal material collected at 0–8 h after dosing.

Figure 1

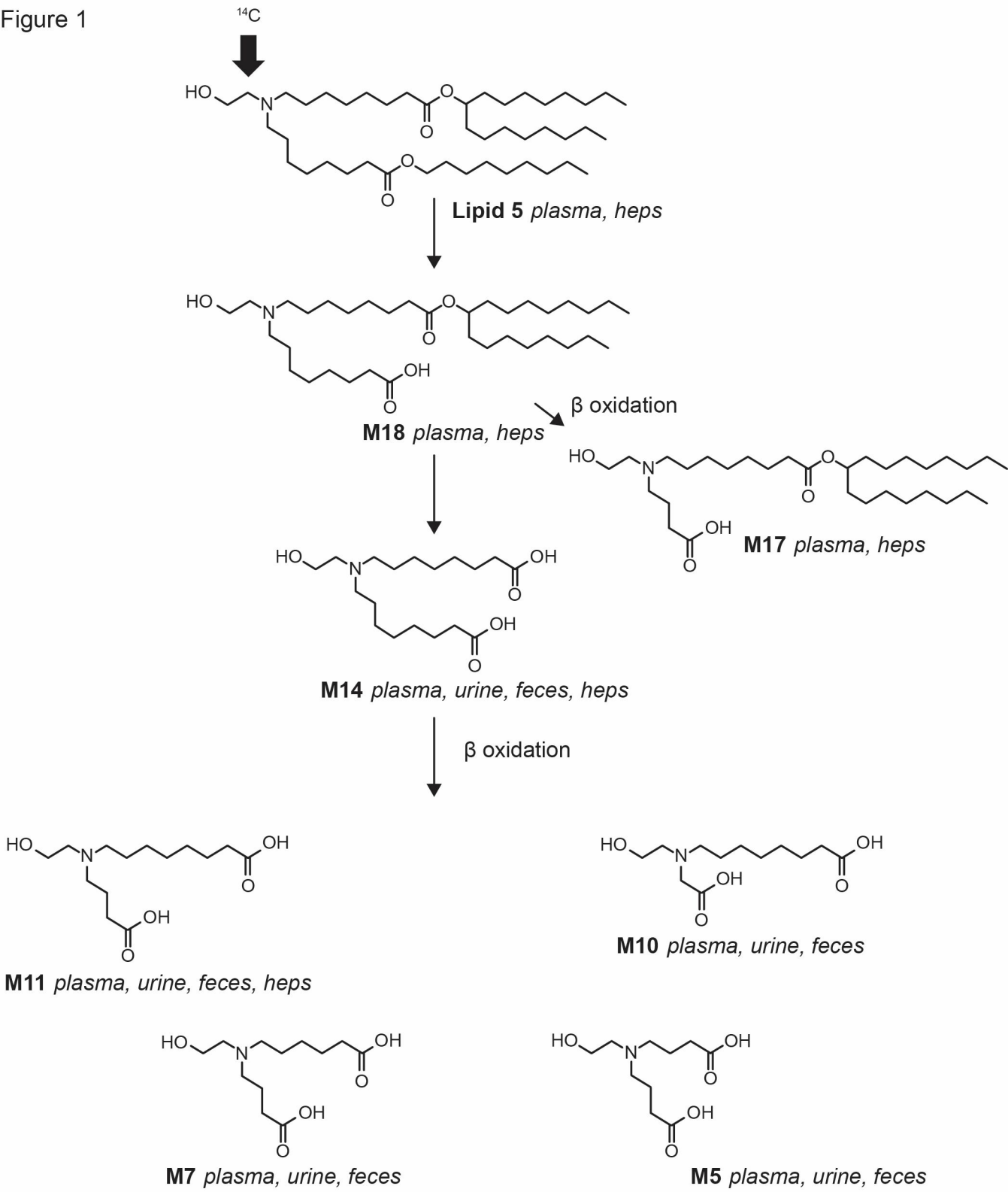
^{14}C
Lipid 5 *plasma, heps*
M18 *plasma, heps*
β oxidation
M17 *plasma, heps*
M14 *plasma, urine, feces, heps*
β oxidation
M11 *plasma, urine, feces, heps*
M10 *plasma, urine, feces*
M7 *plasma, urine, feces*
M5 *plasma, urine, feces*

Figure 2

A

Test Substance	Gender	T_{max} (h)[a]	C_{max} ± SE (ng/mL)	AUC_{last} ± SE (ng/mL*h)	$T_{1/2}$ (h)
[^{14}C]Lipid 5-containing LNPs	Female	0.25	37800 ± 1510	33400 ± 1330	9.04
	Male	0.25	25800 ± 777	24200 ± 2450	8.42

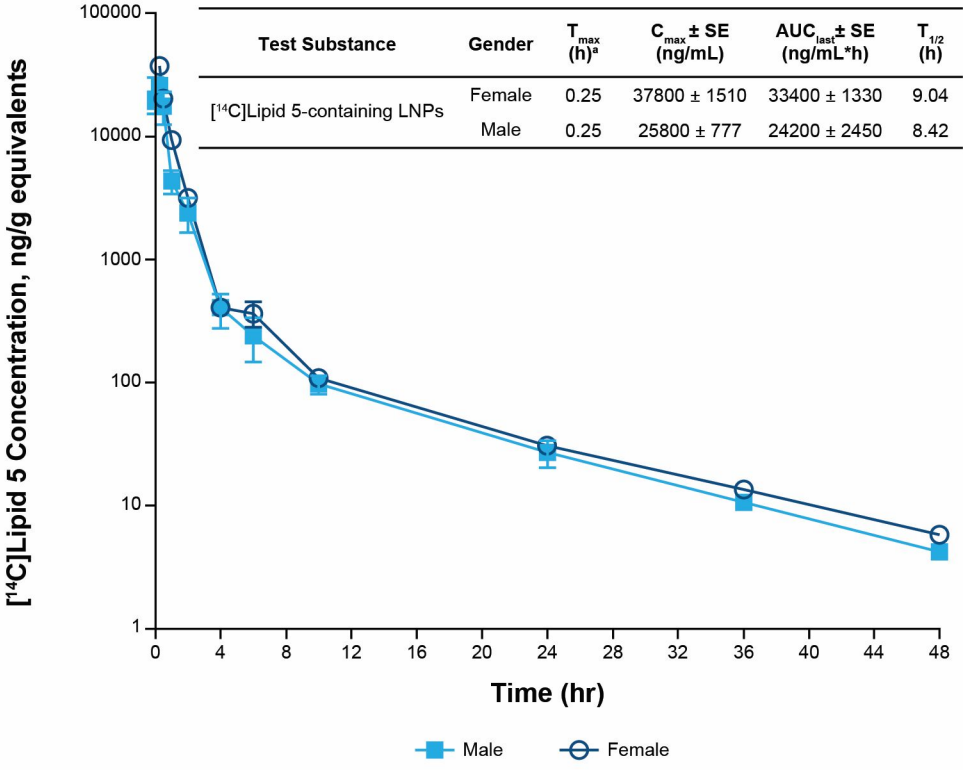

B

Test Substance	Gender	T_{max} (h)[a]	C_{max} ± SE (ng/mL)	AUC_{last} ± SE (ng/mL*h)	$T_{1/2}$ (h)
Lipid 5-containing LNPs	Male	0.16	366000 ± 13500	522000 ± 50700	1.40

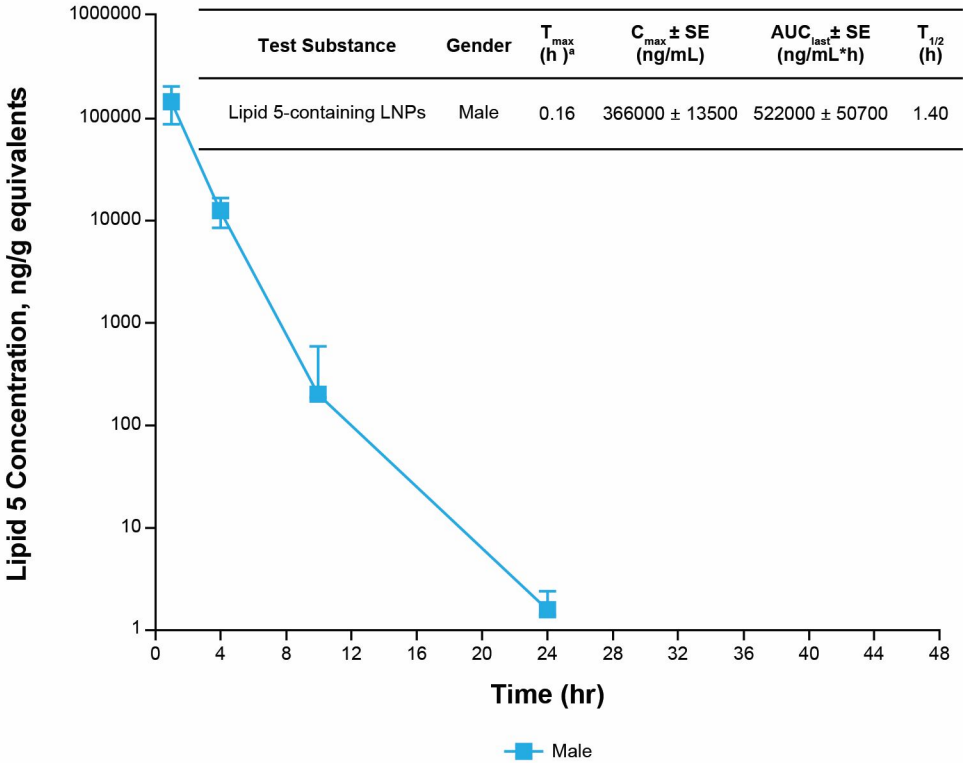

Figure 3

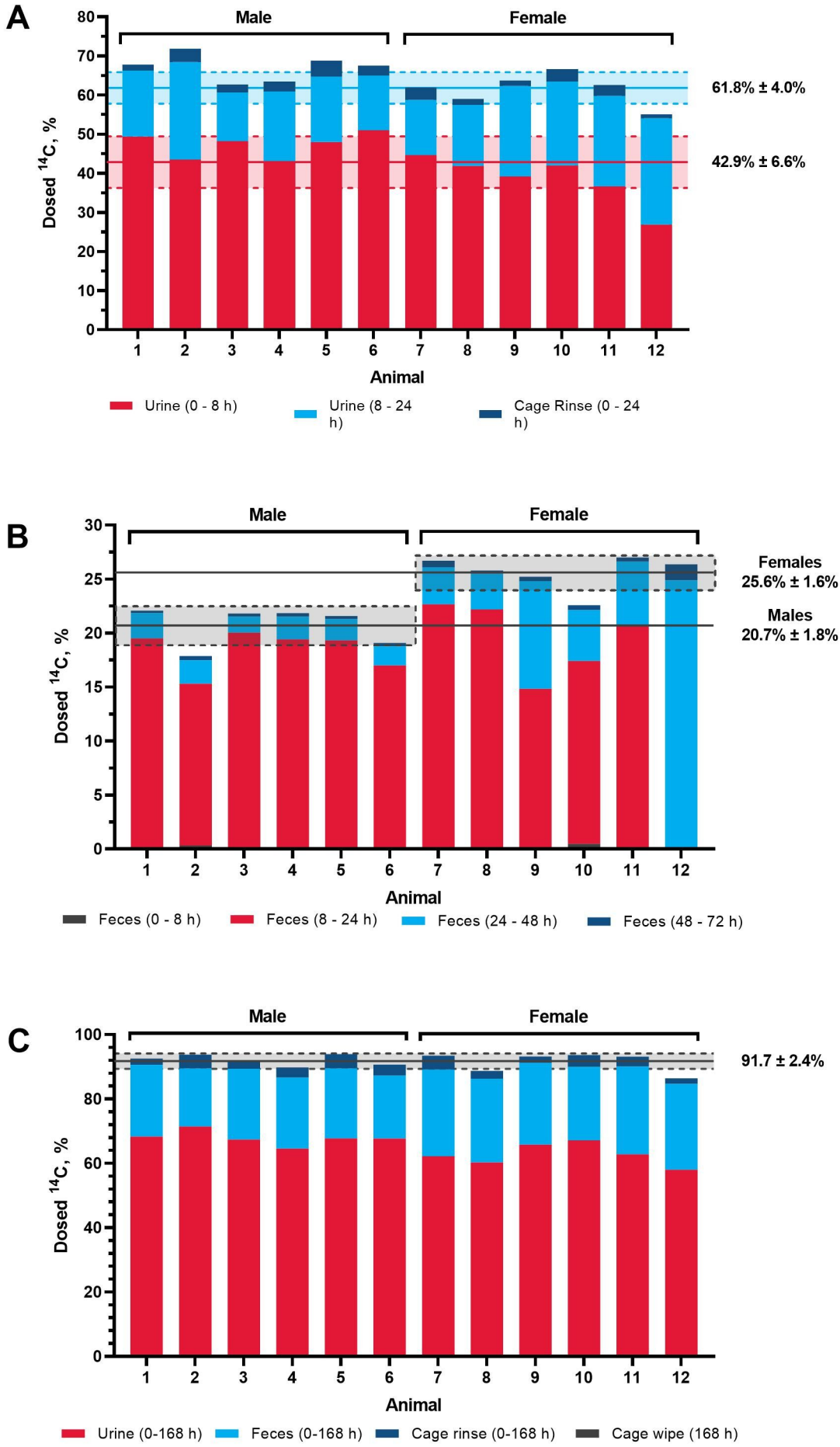
A
Male
Female
Dosed ^{14}C, %
Animal
61.8% ± 4.0%
42.9% ± 6.6%
Urine (0 - 8 h)
Urine (8 - 24 h)
Cage Rinse (0 - 24 h)
B
Male
Female
Dosed ^{14}C, %
Animal
Females
25.6% ± 1.6%
Males
20.7% ± 1.8%
Feces (0 - 8 h)
Feces (8 - 24 h)
Feces (24 - 48 h)
Feces (48 - 72 h)
C
Male
Female
Dosed ^{14}C, %
Animal
91.7 ± 2.4%
Urine (0-168 h)
Feces (0-168 h)
Cage rinse (0-168 h)
Cage wipe (168 h)

Figure 4

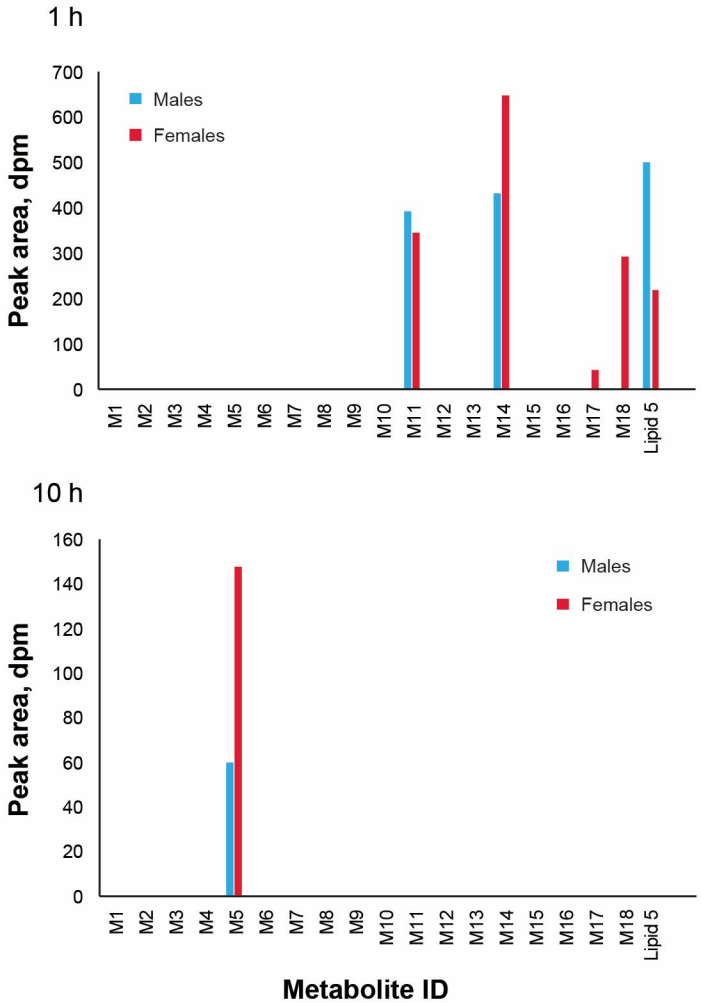
1 h
Peak area, dpm
700
600
500
400
300
200
100
0
Males
Females
M1 M2 M3 M4 M5 M6 M7 M8 M9 M10 M11 M12 M13 M14 M15 M16 M17 M18 Lipid 5
10 h
Peak area, dpm
160
140
120
100
80
60
40
20
0
Males
Females
M1 M2 M3 M4 M5 M6 M7 M8 M9 M10 M11 M12 M13 M14 M15 M16 M17 M18 Lipid 5
Metabolite ID

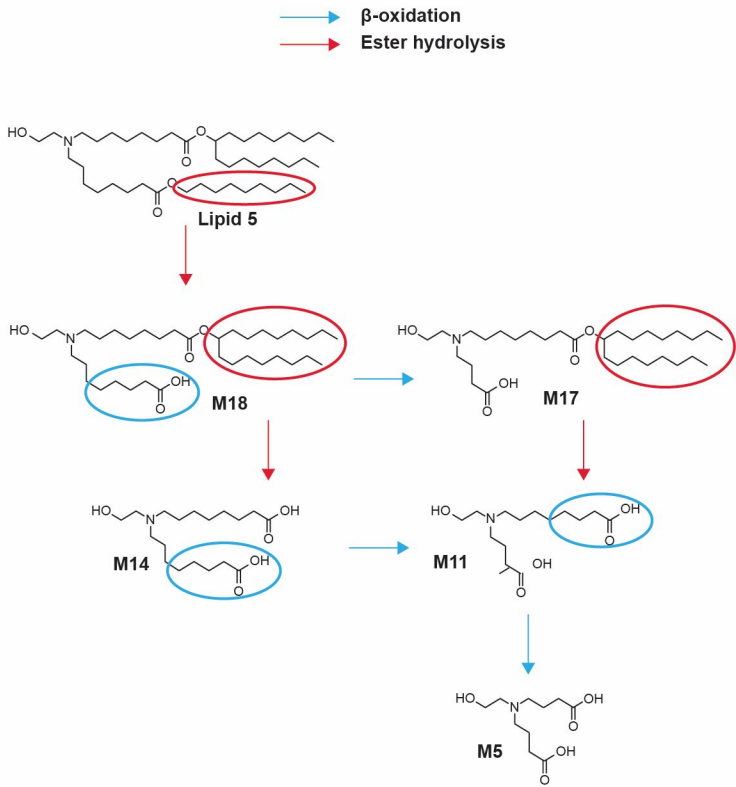
β-oxidation
Ester hydrolysis
Lipid 5
M18
M17
M14
M11
M5

Figure 5

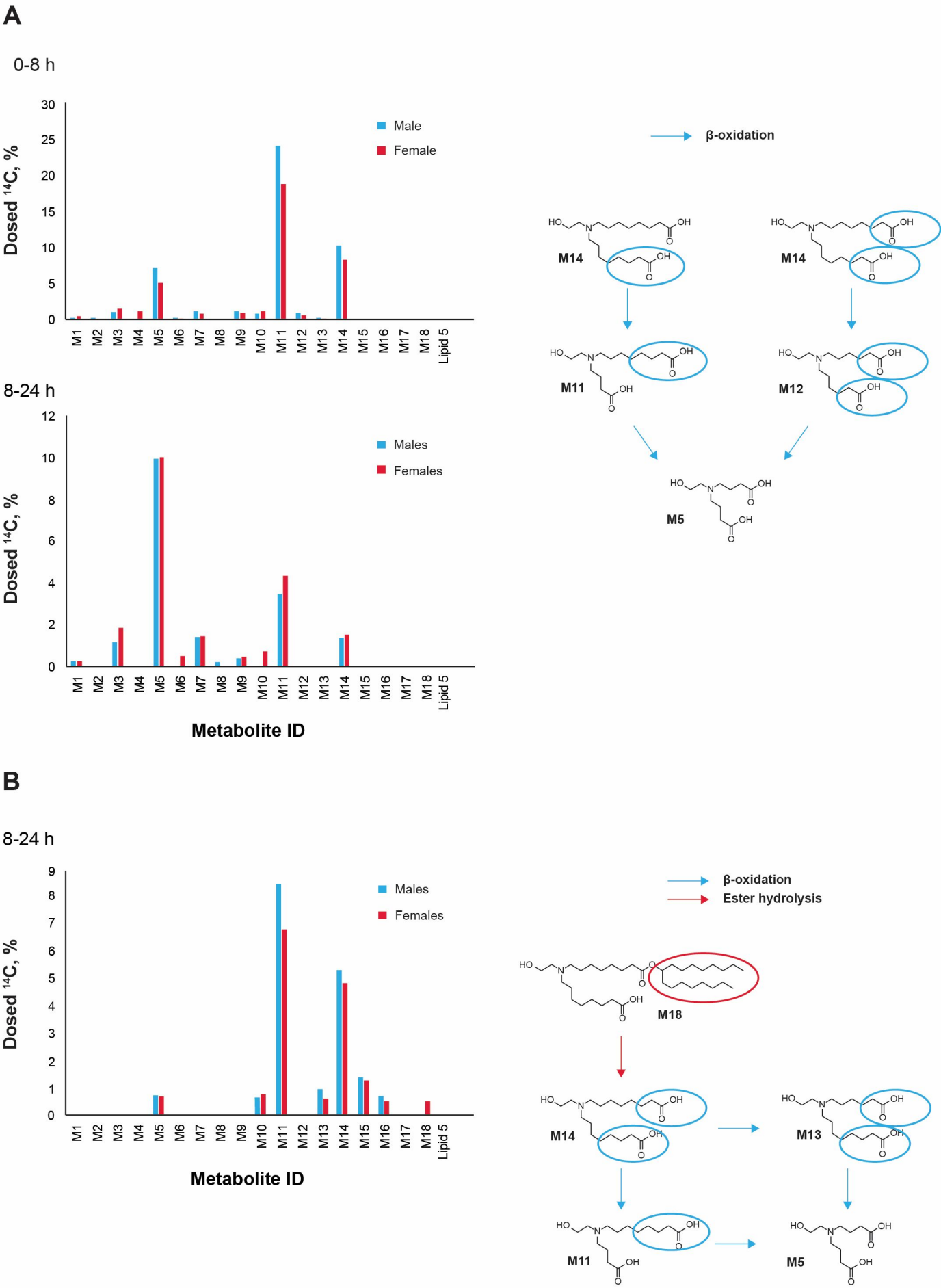
A
0-8 h
Dosed ¹⁴C, %
Male
Female
M1 M2 M3 M4 M5 M6 M7 M8 M9 M10 M11 M12 M13 M14 M15 M16 M17 M18 Lipid 5
8-24 h
Males
Females
Metabolite ID
β-oxidation
M14
M11
M12
M5
B
8-24 h
Ester hydrolysis
M18
M13